

Electroweak Baryogenesis and the Higgs and Stop masses ^{*}Mariano Quirós^a^aInstituto de Estructura de la Materia, Serrano 123 E-28006, Spain

In this talk we review the actual situation concerning electroweak phase transition and baryogenesis in the minimal supersymmetric extension of the Standard Model. A strong enough phase transition requires light Higgs and stop eigenstates. For a Higgs mass in the range 110–115 GeV, there is a stop window in the range 105–165 GeV. If the Higgs is heavier than 115 GeV, stronger constrains are imposed on the space of supersymmetric parameters. A baryon-to-entropy ratio is generated by the chargino sector provided that the μ parameter has a CP-violating phase larger than ~ 0.04 .

1. Introductory remarks

Electroweak baryogenesis [1] is an appealing mechanism to explain the observed, Big Bang Nucleosynthesis (BBN), value of the baryon-to-entropy ratio [2], $\eta_{\text{BBN}} \equiv n_B/s \sim 4 \times 10^{-10}$, at the electroweak phase transition [3], that can be tested at present and future high-energy colliders. Although the Standard Model (SM) contains all the necessary ingredients [1] for a successful baryogenesis, it fails in providing enough baryon asymmetry. In particular it has been proven by perturbative [4] and non-perturbative [5] methods that, for Higgs masses allowed by present LEP bounds [6], the phase transition is too weakly first order, or does not exist at all, and any previously generated baryon asymmetry would be washed out after the phase transition. On the other hand the amount of CP violation arising from the CKM phase is too small for generating the observed baryon asymmetry [7]. Therefore electroweak baryogenesis requires physics beyond the Standard Model at the weak scale.

Among the possible extensions of the Stan-

dard Model at the weak scale, its minimal supersymmetric extension (MSSM) is the best motivated one. It provides a technical solution to the hierarchy problem and has deep roots in more fundamental theories unifying gravity with the rest of interactions. As for the strength of the phase transition [8], a region in the space of supersymmetric parameters has been found [9]–[25] where the phase transition is strong enough to let sphaleron interactions go out of equilibrium after the phase transition and not erase the generated baryon asymmetry. This region (the so-called light stop scenario) provides values of the lightest Higgs and stop eigenstate masses which are being covered at LEP and Tevatron colliders.

The MSSM has new violating phases that can drive enough amount of baryon asymmetry. Several computations have been performed [26]–[38] in recent years, showing that if the CP-violating phases associated with the chargino mass parameters are not too small, these sources may lead to acceptable values of the baryon asymmetry. In this talk I will present some aspects of a recent computation [39] of the CP-violating sources in the chargino sector which improves the computation of Ref. [27] in two main aspects. On the one hand, instead of computing the temporal component of the current in the lowest order of Higgs background insertions, we compute all current

^{*}Based on talks given at: *Strong Electroweak Matter*, Centre de Physique Théorique, Université de Marseille, Marseilles (France), June 14–17, 2000; and, *Thirty years of supersymmetry*, Theoretical Physics Institute, School of Physics and Astronomy, Minneapolis, Minnesota (USA), October 16–27, 2000.

components by performing a resummation of the Higgs background insertion contributions to all order in perturbation theory. The resummation is essential since it leads to a proper regularization of the resonant contribution to the temporal component of the current found in Ref. [27] and leads to contributions which are not suppressed for large values of the charged Higgs mass. On the other hand we consider, in the diffusion equations, the contribution of Higgsino number violating interaction rate [38] from the Higgsino μ term in the lagrangian, Γ_μ , that was considered in our previous calculations in the limit $\Gamma_\mu/T \rightarrow \infty$.

2. The phase transition

The possibility of achieving, in the MSSM, a strong-enough phase transition for not washing out any previously generated baryon asymmetry, characterized by the condition

$$v(T_c)/T_c \gtrsim 1 , \quad (1)$$

has been recently strengthened by three facts:

- The presence of light \tilde{t}_R (with small mixing \tilde{A}_t) considerably enhances the strength of the phase transition [8,9]. This is the so-called light stop scenario.
- Two-loop corrections enhance the phase transition in the SM [4], and in the MSSM [15–17].
- The validity of perturbation theory, and in particular the results of two-loop calculations, for the light stop scenario has been recently confirmed by non-perturbative results [23,24]. In fact, non-perturbative results lead to a stronger phase transition than perturbative ones, by $\sim 10 - 15\%$.

However the price the light stop scenario has to pay is that it may require moderately negative values of the supersymmetric parameter $m_U^2 \equiv -\tilde{m}_U^2$ and then, apart from the electroweak minimum along the Higgs (ϕ) direction, another color breaking minimum along the $U \equiv \tilde{t}_R$ direction might appear. Therefore both directions should be studied at finite temperature.

Table 1
Mass spectrum along the U direction.

field	d.o.f.	mass ²
4 gluons	12	$g_s^2 U^2/2$
1 gluon	3	$2g_s^2 U^2/3$
1 B gauge boson	3	$g'^2 U^2/9$
5 squark-goldstones	5	$m_U^2 + g_s^2 U^2/3$
1 squark	1	$m_U^2 + g_s^2 U^2$
$4 \tilde{Q}_L$ -Higgs	4	$-m_H^2/2 + h_t^2 \sin^2 \beta U^2$
2 Dirac fermions (t_L, \tilde{H})	8	$\mu^2 + h_t^2 U^2$

To systematically analyze the different possibilities we have computed the two-loop effective potential along the ϕ and U directions and compared their cosmological evolutions with T . The two-loop effective potential along the ϕ direction was carefully studied in Ref. [15]. The one-loop correction is dominated by the exchange of the top/stop sector while the two-loop effective potential is given by two-loop diagrams with stops and gluons, as well as one-loop diagrams with the stop thermal counterterm. The two-loop effective potential along the U direction was studied in Refs. [17]. The mass spectrum is given in Table 1, where we have considered small mixing \tilde{A}_t/m_Q and large gluino masses. The one-loop diagrams correspond to the propagation of gluons, squarks and Higgses as well as Dirac fermions. The leading two-loop contributions correspond to sunset and figure-eight diagrams with the fields of Table 1 propagating, as well as one-loop diagrams with thermal counterterm insertions corresponding to gluons and squarks.

For a given value of the supersymmetric parameters we have computed T_c , the critical temperature along the ϕ direction, and T_c^U , the critical temperature along the U direction. Therefore, four different situations can arise:

- a) $T_c^U < T_c$ and $\tilde{m}_U < m_U^c \equiv (m_H^2 v^2 g_s^2/12)^{1/4}$ [9]. In this case the phase transition proceeds first along the ϕ direction and the field remains at the electroweak minimum forever. This region is called *sta-*

bility region.

- **b)** $T_c^U < T_c$ and $\tilde{m}_U > m_U^c$. In this region the electroweak minimum is metastable (*metastability* region). It can be physically acceptable provided that its lifetime is larger than the age of the universe at this temperature: $\Gamma_{\phi \rightarrow U} < H$.
- **c)** $T_c^U > T_c$ and $\tilde{m}_U < m_U^c$. In this case the U -phase transition happens first and therefore it would be physically acceptable provided that the lifetime is shorter than the age of the universe: $\Gamma_{U \rightarrow \phi} > H$. This region is called *two step* region and has been excluded [25].
- **d)** $T_c^U > T_c$ and $\tilde{m}_U > m_U^c$. This is the region of *instability* of the electroweak minimum. It is absolutely excluded.

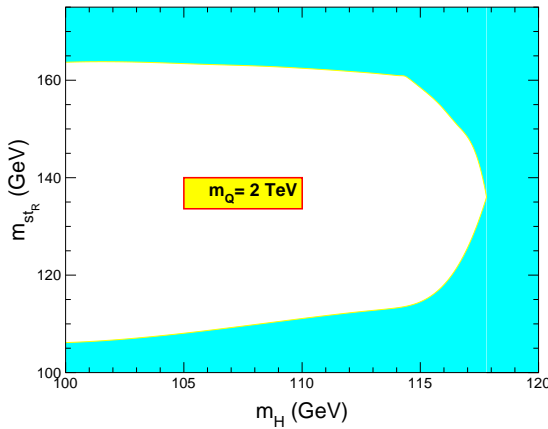


Figure 1. The absolute region of stability in the $(m_H, m_{\tilde{t}_R})$ plane, for $m_Q = 2$ TeV. The allowed region is inside the solid lines.

Fig. 1 shows the absolute region of stability for $m_Q \leq 2$ TeV, where we can see an absolute upper bound on the Higgs mass ~ 117 GeV. In view of the non-perturbative results on the phase transition [5], we have used in Fig. 1 the condition

$v(T_c) \gtrsim 0.9T_c$ in our perturbative two-loop calculation.

3. The CP-violating chargino currents

Our aim in this section is to compute the Green functions for the charged gaugino-Higgsino system \tilde{h}_c - \tilde{W}_c , describing the propagation of these fermions in the presence of a bubble wall. The bubble wall is assumed to be located at the space-time point z , where there is a non-trivial background of the MSSM Higgs fields, $H_i(z)$, which carries dimensionful CP-violating couplings to charginos. We shall use these Green functions to compute the left-handed and right-handed currents corresponding to

$$\psi_R(x) = \begin{pmatrix} \tilde{W}^+ \\ \tilde{h}_2^+ \end{pmatrix}, \quad \psi_L(x) = \begin{pmatrix} \tilde{W}^- \\ \tilde{h}_1^- \end{pmatrix}. \quad (2)$$

at the point z .

Since the mass matrix depends on the space-time coordinates, and we must identify the free and perturbative parts out of it, in order to make such a selection we will expand the mass matrix around the point $z^\mu \equiv (\vec{r}, t)$ (the point where we are calculating the currents in the plasma frame) up to first order in derivatives as,

$$M(x) = M(z) + (x - z)^\mu M_\mu(z), \quad (3)$$

where we use the notation $M_\mu(z) \equiv \partial M(z) / \partial z^\mu$.

The chargino mass matrix in (3) is given by

$$M(z) = \begin{pmatrix} M_2 & u_2(z) \\ u_1(z) & \mu_c \end{pmatrix} \quad (4)$$

where we have defined $u_i(z) \equiv gH_i(z)$. The mass eigenvalues are given by

$$m_1(z) = \frac{(\Delta + \Lambda + u_1^2(z)) M_2 + u_1(z) u_2(z) \mu_c^*}{\sqrt{(\Delta + \Lambda)(\Delta + \Lambda)}} \\ m_2(z) = \frac{(\Delta + \Lambda - u_2^2(z)) \mu_c - u_1(z) u_2(z) M_2}{\sqrt{(\Delta + \Lambda)(\Delta + \Lambda)}}.$$

where field redefinitions have been made in order to make the Higgs vacuum expectation values, as well as the weak gaugino mass M_2 , real, and

$$\begin{aligned} \Delta &= (M_2^2 - |\mu_c|^2 - u_1^2 + u_2^2)/2 \\ \bar{\Delta} &= (M_2^2 - |\mu_c|^2 - u_2^2 + u_1^2)/2 \\ \Lambda &= \left(\Delta^2 + |M_2 u_1 + \mu_c^* u_2|^2 \right)^{1/2} \end{aligned} \quad (5)$$

The vector and axial Higgsino currents can now be defined as:

$$\begin{aligned} j_{H,h}^\mu(z) &= \lim_{x,y \rightarrow z} \{ \text{Tr} [P_2 \sigma^\mu S_\psi^{RR}(x,y;z)] \\ &\pm \text{Tr} [P_2 \bar{\sigma}^\mu S_\psi^{LL}(x,y;z)] \} \end{aligned} \quad (6)$$

where $P_2 = (\sigma_0 - \sigma_3)/2$ is a projection operator and $S_\psi(x,y;z)$ are the Green functions in the weak eigenstate basis after making the expansion (3) and a resummation to all orders in $M(z)$.

The detailed calculation of the currents can be found in Ref. [39]. In particular only the time component is relevant for the diffusion equations of next section where we will use as sources of Higgs densities $\gamma_{H,h} \simeq \Gamma_{\tilde{\mathcal{H}}} j_{H,h}^0(z)$, and $\Gamma_{\tilde{\mathcal{H}}} \sim \alpha_W T$ is the inverse typical thermalization time. In this way we obtain for the vector and axial sources the expressions:

$$\begin{aligned} \gamma_H &\simeq -2 v_\omega g^2 \Gamma_{\tilde{\mathcal{H}}} \text{Im}(M_2 \mu_c) \\ &\quad \{ H^2(z) \beta'(z) [\mathcal{F}(z) + \mathcal{G}(z)] \\ &+ g^2 H^2(z) \cos 2\beta(z) [H(z)H'(z) \sin 2\beta(z) \\ &\quad + H^2(z) \cos 2\beta(z) \beta'(z)] \mathcal{H}(z) \} \end{aligned} \quad (7)$$

$$\begin{aligned} \gamma_h &\simeq 2 v_\omega g^2 \Gamma_{\tilde{\mathcal{H}}} \text{Im}(M_2 \mu_c) \\ &[H(z)H'(z) \sin 2\beta(z) + H^2(z) \cos 2\beta(z) \beta'(z)] \\ &\quad \{ \mathcal{K}(z) + 2(\Delta + \bar{\Delta}) \mathcal{H}(z) \} \end{aligned} \quad .$$

where the functions $\mathcal{F}, \mathcal{G}, \mathcal{H}, \mathcal{K}$ are defined as:

$$\begin{aligned} \mathcal{F}(z) &= \frac{1}{6\pi^2} \text{Re} \int_0^\infty dp^0 (1 + 2f) \\ &\quad \left(\frac{1}{z_1 + z_2} \right)^3 \end{aligned} \quad (8)$$

$$\begin{aligned} \mathcal{G}(z) &= \frac{1}{3\pi^2} \text{Re} \int_0^\infty dp^0 p^0 f' \\ &\left\{ \left(\frac{1}{z_1 + z_2} \right)^3 - \frac{3}{|m_1(z)|^2 - |m_2(z)|^2} \right. \\ &\left[\frac{z_1}{|m_1(z)|^2 - |m_2(z)|^2 - 4i\Gamma_{\tilde{\mathcal{H}}} p^0} \right. \\ &\left. \left. + \frac{z_2}{|m_1(z)|^2 - |m_2(z)|^2 + 4i\Gamma_{\tilde{\mathcal{H}}} p^0} \right] \right\} \end{aligned} \quad (9)$$

$$\begin{aligned} \mathcal{H}(z) &= \frac{1}{8\pi^2} \text{Re} \int_0^\infty dp^0 (1 + 2f) \\ &\quad \frac{1}{z_1 z_2} \left(\frac{1}{z_1 + z_2} \right)^3 \end{aligned} \quad (10)$$

$$\begin{aligned} \mathcal{K}(z) &= -\frac{1}{4\pi^2} \text{Re} \int_0^\infty dp^0 (1 + 2f) \\ &\quad \frac{1}{z_1 z_2} \left(\frac{1}{z_1 + z_2} \right)^3 . \end{aligned} \quad (11)$$

$f \equiv -n_F(|p^0|)$, where n_F is the Fermi-Dirac distribution function and z_i is defined as

$$z_i(p^0) = \sqrt{p^0 \left(p^0 + 2i\Gamma_{\tilde{\mathcal{H}}} \right) - |m_i(z)|^2} \quad (12)$$

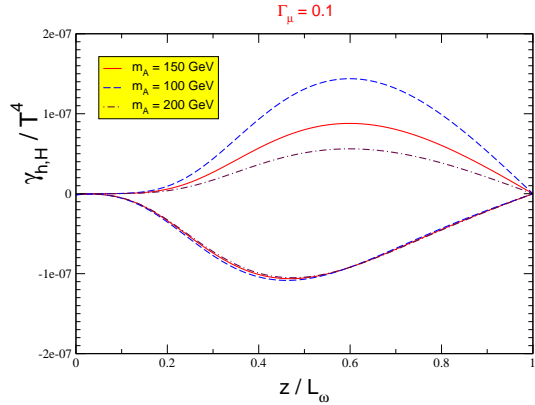


Figure 2. Plot of the sources $\gamma_{H,h}$, for the values of supersymmetric parameters specified in the text, as functions of z/L_ω .

with positive real and imaginary parts satisfying $\text{Re}(z_i) = \Gamma_{\tilde{\mathcal{H}}} p^0 / \text{Im}(z_i)$. Notice that the sources are proportional to the wall velocity v_ω , and so die when the latter goes to zero, which is a physical requirement.

In Fig. 2 we plot the sources $\gamma_{H,h}$ for a chosen set of supersymmetric and bubble parameters. In particular the wall velocity is chosen as $v_\omega = 0.05$ and the bubble wall width as $L_\omega = 20/T$ which is

suggested by detailed numerical analyses of bubble formation [19,40]. For the supersymmetric parameters we choose $m_Q = 1.5$ TeV, $A_t = 0.5$ TeV, $M_2 = \mu = 200$ GeV, $\tan \beta = 20$ and three different values of $m_A = 100, 150, 200$ GeV, corresponding to the dashed, solid and dot-dashed curves of Fig. 2. From it we can see two main features. On the one hand, γ_H is very sensitive to the value of m_A , and so to the corresponding value of $\Delta\beta$, as expected, and decreases when m_A increases. On the other hand, γ_h is dominant only for large values of m_A , such that the $\Delta\beta$ suppression of γ_H is stronger. But it is never overwhelming the contribution of γ_H , because it is $\tan \beta$ suppressed.

We also computed the bubble solutions of the MSSM [19] using the two-loop effective potential and we have confirmed the goodness of the thick wall approximation ($L_\omega T_c \gg 10 v_\omega$).

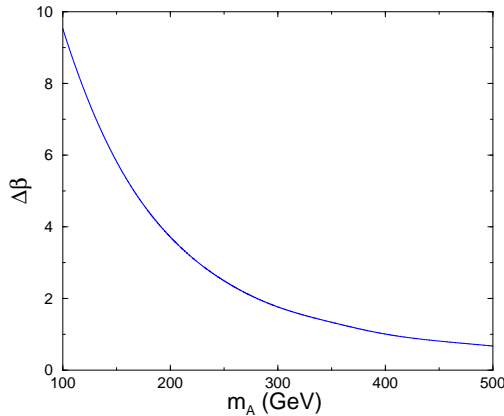


Figure 3. $\Delta\beta$, in units of 10^{-3} , as a function of m_A for the values of the supersymmetric and bubble parameters indicated in the text.

In Fig. 3, we plot $\Delta\beta(T)$ for the following values of the supersymmetric: $M_2 = \mu = 200$ GeV, $A_t = 500$ GeV, $m_Q = 1.5$ TeV. Notice that the value of T_c , as well as $\Delta\beta$, is different from point to point, for different values of m_A . We see from

Fig. 3 that $\Delta\beta$ goes from $\sim 10^{-2}$ for $m_A = 100$ GeV, to $\sim 10^{-3}$ for $m_A = 500$ GeV. This fact will have an important impact on the mechanism of baryon asymmetry.

4. The diffusion equations

To evaluate the baryon asymmetry generated in the broken phase we need to first compute the density of left-handed quarks and leptons, n_L , in front of the bubble wall (in the symmetric phase). These chiral densities are the ones that induce weak sphalerons to produce a net baryon number. Since, in the present scenario, there is essentially no lepton asymmetry, the density to be computed in the symmetric phase is $n_L = n_Q + \sum_{i=1}^2 n_{Q_i}$ where the density of a chiral supermultiplet $Q \equiv (q, \tilde{q})$ is understood as the sum of densities of particle components, assuming the supergauge interactions to be in thermal equilibrium, $n_Q = n_q + n_{\tilde{q}}$. If the system is near thermal equilibrium, particle densities, n_i , are related to the local chemical potential, μ_i by the relation $n_i = k_i \mu_i T^2 / 6$, where k_i are statistical factors equal to 2 (1) for bosons (fermions). In fact, assuming that all quarks have nearly the same diffusion constant it turns out that [26], $n_L = 5 n_Q + 4 n_T$.

One can write now a set of diffusion equations involving n_Q , n_T , n_{H_1} (the density of $H_1 \equiv (h_1, \tilde{h}_1)$) and n_{H_2} (the density of $\bar{H}_2 \equiv (\bar{h}_2, \tilde{\bar{h}}_2)$), and the particle number changing rates and CP-violating source terms discussed above. In the bubble wall frame, and ignoring the curvature of the bubble wall, all quantities become functions of $z \equiv r + v_\omega t$. In the limit of fast Yukawa coupling Γ_Y and strong sphaleron Γ_{ss} rates, we can write the diffusion equations as:

$$\begin{aligned}
 v_\omega [n'_Q + 2n'_T - n'_H] &= D_q [n''_Q + 2n''_T] \\
 -D_h n''_H + \Gamma_m \left[\frac{n_Q}{k_Q} - \frac{n_T}{k_T} \right] \Gamma_h \frac{n_H}{k_H} - \gamma_H \\
 v_\omega [n'_Q + 2n'_T - n'_h] &= D_q [n''_Q + 2n''_T] \\
 -D_h n''_h + \Gamma_m \left[\frac{n_Q}{k_Q} - \frac{n_T}{k_T} \right] \\
 + [\Gamma_h + 4\Gamma_\mu] \frac{n_h}{k_H} - \gamma_h . \tag{13}
 \end{aligned}$$

where n_Q and n_T are replaced by the (approximate) explicit solutions

$$\begin{aligned} n_Q &= \frac{k_Q(9k_T - k_B)}{k_H(k_B + 9k_Q + 9k_T)} (n_H + n_h) \\ n_T &= -\frac{k_T(9k_Q + 2k_B)}{k_H(k_B + 9k_Q + 9k_T)} (n_H + n_h) \end{aligned} \quad (14)$$

$D_q \sim 6/T$ and $D_h \sim 110/T$ are the corresponding diffusion constants in the quark and Higgs sectors, $n_H \equiv n_{H_2} + n_{H_1}$, $n_h \equiv n_{H_2} - n_{H_1}$, $k_H \equiv k_{H_1} + k_{H_2}$, and Γ_μ corresponds to the $\mu_c \tilde{H}_1 \tilde{H}_2$ term in the Lagrangian. There are also the Higgs number violating and axial top number violation processes, induced by the Higgs self interactions and by top quark mass effects, with rates Γ_h and Γ_m , respectively, that are only active in the broken phase.

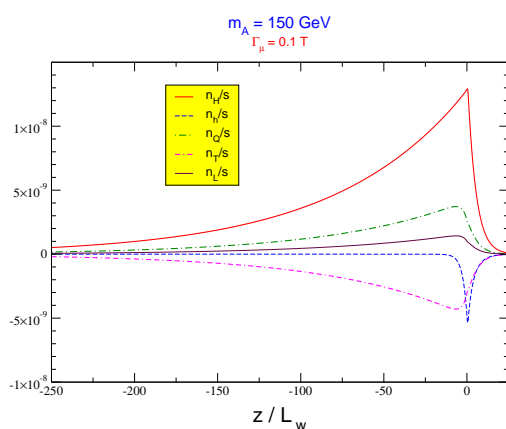


Figure 4. Plot of the different density-to-entropy ratios for the values of supersymmetric parameters specified in the text.

The system of equations (13) has been solved numerically in Ref. [39], where also a good enough analytical approximation is provided. In Fig. 4 we plot the numerical solution corresponding to the same set of supersymmetric and bubble parameters as in Fig. 2. All densities diffuse along the

symmetric phase ($z < 0$), where weak sphalerons are active, which is essential for the left-handed quark asymmetry to bias the weak sphalerons to violate baryon number. In particular, we can see from Fig. 4 that the density n_H is larger than n_h , for $\Gamma_\mu = 0.1 T$. In previous analyses [26,27] the limit $\Gamma_\mu \rightarrow \infty$ was implicitly assumed and n_h was completely neglected. Fig. 4 shows that this is not such a bad approximation. Furthermore, the relative importance of n_H and n_h is shown for different values of $\Gamma_\mu = 0.01 T, 0.1 T, T$ in Fig. 5. We can see that while for $\Gamma_\mu = 0.01 T$ n_h is sizeable, for $\Gamma_\mu = T$ it is negligible in good agreement with our previous results [27].

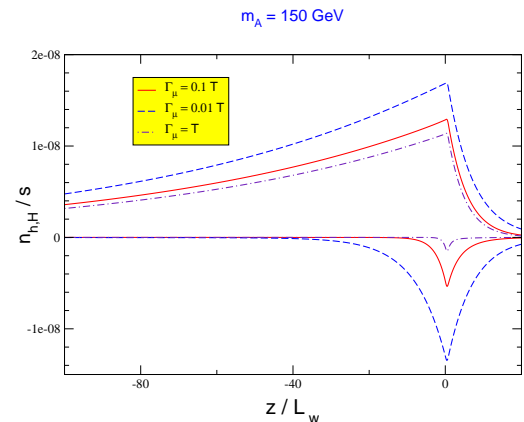


Figure 5. Plots of densities-to-entropy ratios $n_{H,h}/s$ as functions of z/L_ω for different values of Γ_μ .

5. The baryon asymmetry

In this section we present the numerical results of the baryon asymmetry computed in the previous section and, in particular, of the baryon-to-entropy ratio $\eta \equiv n_B/s$, where the entropy density is given by $s = \frac{2\pi^2}{45} g_{eff} T^3$, with g_{eff} being the effective number of relativistic degrees of freedom.

Since we assume the sphalerons are inactive inside the bubbles, the baryon density is constant in the broken phase and satisfies, in the symmetric phase, an equation where n_L acts as a source [26] and there is an explicit sphaleron-induced relaxation term [39]

$$v_\omega n'_B(z) = -\theta(-z) [n_F \Gamma_{ws} n_L(z) + \mathcal{R} n_B(z)] \quad (15)$$

where $n_F = 3$ is the number of families and $\mathcal{R} = \frac{5}{4} n_F \Gamma_{ws}$ is the relaxation coefficient. Eq. (15) can be solved analytically and gives, in the broken phase $z \geq 0$, a constant baryon asymmetry,

$$n_B = -\frac{n_F \Gamma_{ws}}{v_\omega} \int_{-\infty}^0 dz n_L(z) e^{z\mathcal{R}/v_\omega}. \quad (16)$$

The profiles $H(z)$, $\beta(z)$ have been accurately computed in the literature [19]. For the sake of simplicity, in this work we use a kink approximation

$$H(z) = \frac{1}{2} v(T) \left(1 - \tanh \left[\alpha \left(1 - \frac{2z}{L_\omega} \right) \right] \right) \quad (17)$$

$$\beta(z) = \beta - \frac{1}{2} \Delta\beta \left(1 + \tanh \left[\alpha \left(1 - \frac{2z}{L_\omega} \right) \right] \right).$$

This approximation has been checked to reproduce the exact calculation of the Higgs profiles within a few percent accuracy, provided that we borrow from the exact calculation the values of the thickness $L_\omega/2\alpha$ and the variation of the angle $\beta(z)$ along the bubble wall, $\Delta\beta$, as we will do. In particular we will take $\alpha = 3/2$, $L_\omega = 20/T$, and we have checked that the result varies only very slowly with those parameters, while we are taking the values of $\Delta\beta$ which are obtained from the two-loop effective potential used in our calculation.

In Fig. 6 we have fixed $\eta = \eta_{\text{BBN}}$ and plot $\sin \varphi_\mu$, where φ_μ is defined as $\mu_c = \mu \exp(i\varphi_\mu)$, as a function of μ . We have fixed all bubbles and supersymmetric parameters as in Fig. 2, fixed $M_2 = \mu$ and ran over three typical values of the pseudoscalar Higgs mass m_A . In all cases the phase transition is strong enough first order, $v(T_c)/T \simeq 1$, the running mass of the lightest

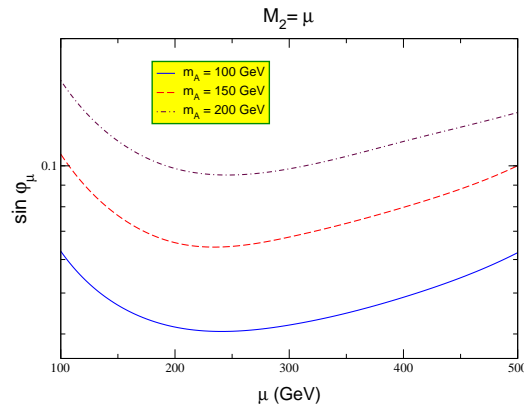


Figure 6. Plot of $\sin \varphi_\mu$ as a function of $M_2 = \mu$ for the values of supersymmetric parameters specified in the text.

stop is around 120 GeV and the Higgs mass is, within the accuracy of our calculations, between 110 and 115 GeV.

Since the computed η behaves almost linearly in $\sin \varphi_\mu$, and we have fixed $\eta = \eta_{\text{BBN}}$, the more baryon asymmetry is generated the smaller the value of $\sin \varphi_\mu$. This can be seen from Fig. 6 where we have been working at the resonance peak $M_2 = \mu$ and hence baryogenesis has been maximized. We see, for all values of m_A , that the minimum of $\sin \varphi_\mu$ sits around $\mu \simeq 200$ GeV. The value of $\sin \varphi_\mu$ at the minimum decreases with m_A . In particular, for $m_A \simeq 100$ GeV, which is about the lower limit from present LEP data (in fact, the present preliminary bounds from LEP [6] are $m_A > 89.9$ GeV for large values of $\tan \beta$, as those we are using in our plots) we obtain that $\sin \varphi_\mu \gtrsim 0.04$. The dependence of $\sin \varphi_\mu$ with respect to supersymmetric and bubble parameters, as $M_2 \neq \mu$, m_A and v_ω has been thoroughly analyzed in Ref. [39] where the reader can find it as well as details of the calculation of supersymmetric chargino sources.

6. Conclusions

The main conclusion after a detailed analysis of both the phase transition and the baryogenesis mechanism in the MSSM is that it is still alive after the recent experimental results at high-energy colliders and, in particular, at the LEP collider.

Concerning the phase transition, its strength is controlled mainly by the Higgs mass and the lightest (right-handed) stop mass. Bubbles are formed with thick walls (the value of the thickness is $\sim L_\omega/3$, with $L_\omega \sim 20/T$) and propagate with extremely non-relativistic velocities ($v_\omega \sim 0.1 - 0.01$). The strength of the phase transition has to be such that $v(T) \gtrsim T$ at the critical temperature. This imposes a strong constraint on the supersymmetric parameters in order to avoid sphaleron erasure, in particular in view of the most recent (preliminary) bounds on the SM-like Higgs mass, $m_H > 113.2$ GeV and the observed excess of events with $b\bar{b}$ invariant mass ~ 114 GeV. Here two possibilities can be drawn:

- The observed excess of events corresponds to a Higgs signal.

In this case the combined Higgs mass and BAU requirements impose some restrictions on the supersymmetric parameters.

a) Heavy pseudoscalars and large $\tan\beta$: say $m_A > 150$ GeV and $\tan\beta > 5$;
b) Heavy left-handed stops and controlled stop mixing: $m_Q \gtrsim 1$ TeV and $0.25 \lesssim A_t/m_Q \lesssim 0.4$; and, **c)** Light right-handed stops: $105 \text{ GeV} \lesssim m_{\tilde{t}} \lesssim 165 \text{ GeV}$. In this case the first prediction of the BAU scenario would have been realized and we would need confirmation for the rest, in particular for the light stop.

- The observed excess of events does not correspond to a Higgs signal.

In that case a reduction of the $Hb\bar{b}$ coupling would be needed. For the values of A_t and μ consistent with electroweak baryogenesis, a reduction of the coupling of the CP-even Higgs boson to the bottom quark would demand not only small values of $m_A \simeq 100 - 150$ GeV, but also large values of $\tan\beta > 10$

and of $|\mu A_t|/m_Q^2 > 0.1$ (the larger $\tan\beta$, the easier suppressed values of the bottom quark coupling are obtained). A detailed discussion on this issue has already been done [39].

Finally, concerning the generated baryon asymmetry, we have found that it requires the CP-violating phase to be, $\varphi_\mu \gtrsim 0.04$. Values of $\varphi_\mu \gtrsim 0.04$ can lead to acceptable phenomenology if either peculiar cancellations in the squark and slepton contributions to the neutron and electron electric dipole moments (EDM) occur [41], and/or if the first and second generation of squarks are heavy. This second possibility is quite appealing and, as has been recently demonstrated [42], leads to acceptable phenomenology.

Acknowledgments

I would like to thank M. Carena, J.M. Moreno, M. Seco and C.E.M. Wagner for the intensive collaboration on the subject during the last year. This work has been supported in part by CICYT, Spain, under contract AEN98-0816, and by EU under contract HPRN-CT-2000-00152.

REFERENCES

1. A.D. Sakharov, “Violation Of CP Invariance, C Asymmetry, And Baryon Asymmetry Of The Universe,” *Pisma Zh. Eksp. Teor. Fiz.* **5** (1967) 32.
2. K.A. Olive, G. Steigman and T.P. Walker, *Phys. Rep.* **333-334** (2000) 389.
3. For reviews, see: A.G. Cohen, D.B. Kaplan and A.E. Nelson, *Annu. Rev. Nucl. Part. Sci.* **43** (1993) 27; M. Quirós, *Helv. Phys. Acta* **67** (1994) 451; M. Quirós, “Finite temperature field theory and phase transitions,” hep-ph/9901312; V.A. Rubakov and M.E. Shaposhnikov, *Phys. Usp.* **39** (1996) 461; M. Carena and C.E.M. Wagner, hep-ph/9704347; A. Riotto, M. Trodden, *Ann. Rev. Nucl. Part. Sci.* **49** (1999) 35; M. Quirós and M. Seco, *Nucl. Phys. B Proc. Suppl.* **81** (2000) 63, hep-ph/9703274.
4. G.W. Anderson and L.J. Hall, *Phys. Rev. D* **45** (1992) 2685; M.E. Carrington,

Phys. Rev. **D45** (1992) 2933; M. Dine, R.G. Leigh, P. Huet, A. Linde and D. Linde, *Phys. Lett.* **B283** (1992) 319; *Phys. Rev.* **D46** (1992) 550; P. Arnold, *Phys. Rev.* **D46** (1992) 2628; J.R. Espinosa, M. Quirós and F. Zwirner, *Phys. Lett.* **B314** (1993) 206; W. Buchmüller, Z. Fodor, T. Helbig and D. Walliser, *Ann. Phys.* **234** (1994) 260; J. Bagnasco and M. Dine, *Phys. Lett.* **B303** (1993) 308; P. Arnold and O. Espinosa, *Phys. Rev.* **D47** (1993) 3546; Z. Fodor and A. Hebecker, *Nucl. Phys.* **B432** (1994) 127.

5. K. Jansen, *Nucl. Phys. Proc. Suppl.* **47** (1996) 196 [hep-lat/9509018]; K. Rummukainen, M. Tsypin, K. Kajantie, M. Laine and M. Shaposhnikov, *Nucl. Phys.* **B532** (1998) 283; K. Rummukainen, K. Kajantie, M. Laine, M. Shaposhnikov and M. Tsypin, hep-ph/9809435.

6. R. Barate *et al.* [ALEPH Collaboration], “Observation of an excess in the search for the standard model Higgs boson at ALEPH,” hep-ex/0011045; M. Acciarri *et al.* [L3 Collaboration], “Higgs candidates in $e^+ e^-$ interactions at $s^{**}(1/2) = 206.6$ -GeV,” hep-ex/0011043.

7. G.R. Farrar and M.E. Shaposhnikov, *Phys. Rev. Lett.* **70** (1993) 2833; (E): **71** (1993) 210 and *Phys. Rev.* **D50** (1994) 774; G. R. Farrar and M. E. Shaposhnikov, “Note added to ‘Baryon asymmetry of the universe in the standard model’,” hep-ph/9406387. M.B. Gavela, P. Hernández, J. Orloff, O. Pène and C. Quimbay, *Mod. Phys. Lett.* **9** (1994) 795; *Nucl. Phys.* **B430** (1994) 382; P. Huet and E. Sather, *Phys. Rev.* **D51** (1995) 379.

8. J.R. Espinosa, M. Quirós and F. Zwirner, *Phys. Lett.* **B307** (1993) 106; A. Brignole, J.R. Espinosa, M. Quirós and F. Zwirner, *Phys. Lett.* **B324** (1994) 181.

9. M. Carena, M. Quirós and C.E.M. Wagner, *Phys. Lett.* **B380** (1996) 81.

10. D. Delepine, J.M. Gérard, R. González Felipe and J. Weyers, *Phys. Lett.* **B386** (1996) 183.

11. J.M. Moreno, D.H. Oaknin and M. Quirós, *Nucl. Phys.* **B483** (1997) 267; *Phys. Lett.* **B395** (1997) 234.

12. J. Cline and K. Kainulainen, *Nucl. Phys.* **B482** (1996) 73; *Nucl. Phys.* **B510** (1998) 88.

13. M. Laine, *Nucl. Phys.* **B481** (1996) 43.

14. M. Losada, *Phys. Rev.* **D56** (1997) 2893; G. Farrar and M. Losada, *Phys. Lett.* **B406** (1997) 60.

15. J.R. Espinosa, *Nucl. Phys.* **B475** (1996) 273; B. de Carlos and J.R. Espinosa, *Nucl. Phys.* **B503** (1997) 24.

16. D. Bodeker, P. John, M. Laine and M.G. Schmidt, *Nucl. Phys.* **B497** (1997) 387.

17. M. Carena, M. Quirós and C.E.M. Wagner, *Nucl. Phys.* **B524** (1998) 3.

18. M. Laine and K. Rummukainen, *Nucl. Phys.* **B535** (1998) 423.

19. J.M. Moreno, M. Quirós and M. Seco, *Nucl. Phys.* **B526** (1998) 489.

20. J.M. Cline and G.D. Moore *Phys. Rev. Lett.* **81** (1998) 3315.

21. P. John, *Phys. Lett.* **B452** (1999) 221.

22. M. Losada, *Nucl. Phys.* **B537** (1999) 3, *Nucl. Phys.* **B569** (2000) 125; M. Laine and M. Losada, *Nucl. Phys.* **B582** (2000) 277.

23. F. Csikor, Z. Fodor, P. Hegedus, A. Jakovac, S.D. Katz and A. Piroth, *Phys. Rev. Lett.* **85** (2000) 932.

24. M. Laine and K. Rummukainen, hep-lat/0009025.

25. J.M. Cline, G.D. Moore and G. Servant, *Phys. Rev.* **D60** (1999) 105035.

26. P. Huet and A.E. Nelson, *Phys. Lett.* **B355** (1995) 229; *Phys. Rev.* **D53** (1996) 4578.

27. M. Carena, M. Quiros, A. Riotto, I. Vilja and C.E.M. Wagner, *Nucl. Phys.* **B503** (1997) 387.

28. J. Cline, M. Joyce and K. Kainulainen, *Phys. Lett.* **B417** (1998) 79, Erratum-ibid. **B448** (1999) 321.

29. T. Multamaki, I. Vilja, *Phys. Lett.* **B411** (1997) 301.

30. A. Riotto, *Int. J. Mod. Phys.* **D7** (1998) 815, *Nucl. Phys.* **B518** (1998) 339, *Phys. Rev.* **D58** (1998) 095009.

31. M.P. Worah, *Phys. Rev.* **D56** (1997) 2010, *Phys. Rev. Lett.* **79** (1997) 3810.

32. H. Davoudiasl, K. Rajagopal and E. Westphal, *Nucl. Phys.* **B515** (1998) 384.

33. J.M. Cline, M. Joyce and K. Kainulainen, *Phys. Lett.* **B417** (1998) 79, Erratum-*ibid.* **B448** (1999) 321.
34. K. Enqvist, A. Riotto and I. Vilja, *Phys. Lett.* **B438** (1998) 273.
35. M. Trodden, *Rev. Mod. Phys.* **71** (1999) 1463.
36. N. Rius and V. Sanz, *Nucl. Phys.* **B570** (2000) 155.
37. M. Brhlik, G.J. Good and G.L. Kane, *Phys. Rev.* **D63** (2001) 035002 [hep-ph/9911243].
38. J.M. Cline and K. Kainulainen, *Phys. Rev. Lett.* **85** (2000) 5519 [hep-ph/0002272]; J.M. Cline, M. Joyce and K. Kainulainen, *JHEP* **07** (2000) 018.
39. M. Carena, J.M. Moreno, M. Quiros, M. Seco and C.E.M. Wagner, hep-ph/0011055.
40. G. D. Moore, *JHEP* **0003** (2000) 006 [hep-ph/0001274]; P. John and M. G. Schmidt, hep-ph/0002050.
41. T. Ibrahim and P. Nath, *Phys. Lett.* **B418** (1998) 98; *Phys. Rev.* **D57** (1998) 478; (E) **D58** (1998) 019901; *Phys. Rev.* **D58** (1998) 111301; (E) **D60** (1999) 099902; M. Brhlik, G.J. Good and G.L. Kane, *Phys. Rev.* **D59** (1999) 115004.
42. See J. Feng, K. Matchev and F. Wilczek, *Phys. Lett.* **B482** (2000) 388.